

Regioregular and Regioirregular Oligoether Carbonates: A $^{13}\text{C}\{^1\text{H}\}$ NMR Investigation

Matthew J. Byrnes, Malcolm H. Chisholm,* Christopher M. Hadad,* and Zhiping Zhou

Department of Chemistry, The Ohio State University, 100 W. 18th Avenue, Columbus, Ohio 43210

Received January 22, 2004; Revised Manuscript Received March 5, 2004

ABSTRACT: Oligoether carbonates $\text{R}(\text{PO})_n\text{OCO}_2(\text{PO})_m\text{R}$, where $\text{R} = \text{Me, Et, or H}$, $\text{PO} =$ propylene oxide ring-opened unit, and $n = 1, 2, 3, 4, \sim 10$, and ~ 30 , have been prepared and characterized by ESI/MS or MALDI/MS and $^{13}\text{C}\{^1\text{H}\}$ NMR spectroscopy in addition to ^1H NMR, DEPT, COSY, and HMQC. The propylene oxide (PO) units have been derived from *S*-PO and *rac*-PO. The compounds have been examined as potential models for polyether carbonate units in poly(propylene carbonate). For HH junctions, assignments of isotactic (*i*) and syndiotactic (*s*) diads and *iii*, *iis/sii*, *sis*, *isi*, *ssi/iss*, and *sss* tetrads are unequivocal. Assignments at the hexad level are limited. For higher oligoether carbonates, i.e., $n \sim 10$ or ~ 30 , only the *i* and *s* diad sensitivity is possible at 150 MHz $^{13}\text{C}\{^1\text{H}\}$ NMR. Calculations on the compounds $\text{MeOCH}_2\text{CHMeOCO}_2\text{CHMeCH}_2\text{OMe}$ (*RR* (*i*) and *SR* (*s*)) and $\text{MeOCO}_2\text{CH}_2\text{CHMeOCO}_2\text{CHMeCH}_2\text{OCO}_2\text{Me}$ were carried out employing density functional theory (DFT) at the B3LYP/6-31G(d) level for geometry optimization and the B3LYP/6-311+G(2d,p) level for NMR calculations. These results are compared with the experimental work and structures of dimethyl carbonate.

Introduction

There is an increasing interest in the synthesis of polycarbonates by environmentally friendly routes, such as in the copolymerization of epoxides (oxiranes) and carbon dioxide.^{1–3} This might provide an alternative to condensation polymerization involving phosgene and diols.⁴ The copolymerization of propylene oxide and carbon dioxide by certain metal catalysts has been known for some time as shown below,⁵ though these processes are not very efficient and, as such, do not offer commercial attraction.⁶ However, recent studies have suggested that these problems may be overcome by appropriate catalyst modification.^{7–10} In our studies of poly(propylene carbonate), PPC, we have found that different catalyst systems yield markedly different polymers as deduced by high field NMR studies. A common impurity in certain samples of PPC is the occurrence of ether-rich segments. As shown in Figure 1, the $^{13}\text{C}\{^1\text{H}\}$ signals in the carbonate region reveal the existence of carbonate carbons flanked by more than one ether unit.^{11,12} Inasmuch as the regio- and stereochemistry of a polymer bears a memory of the reaction pathway leading to its formation, we were struck by the fact that we had little or no basis upon which to assign these carbonate signals. We were thus prompted to synthesize some model compounds and report herein the findings of these studies.



Results and Discussion

Synthesis. The general synthetic route to these ether carbonates is shown in Scheme 1.^{13–15} The etherols $\text{Et}(\text{OCH}_2\text{CHMe})_n\text{OH}$, where $n = 1, 2, 3$, and 4, were separated by spinning band column distillation. For $n = 2, 3$, and 4, the distillations were carried out under reduced pressure. The ring-opening of propylene oxide (PO) in Scheme 1 involves backside attack, and by

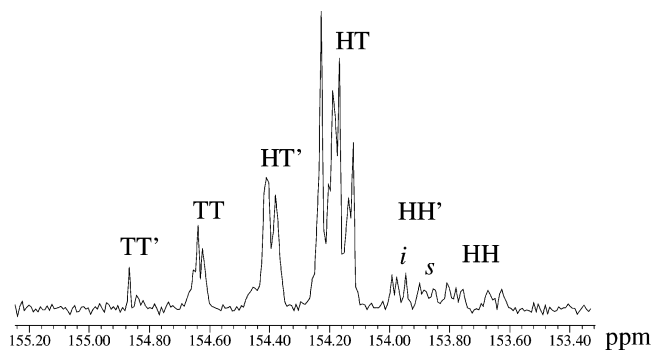
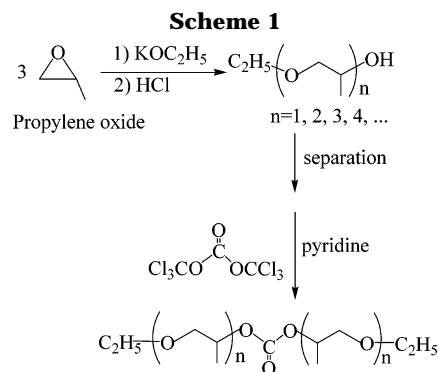


Figure 1. $^{13}\text{C}\{^1\text{H}\}$ (150 MHz, CDCl_3) NMR spectra of carbonate carbon region of PPC made from *rac*-PO employing the $(\text{TPP})\text{AlCl}/\text{EtPh}_3\text{PBr}$ catalytic system. HH' , HT' , and TT' are ether-rich carbonate signals. The *i* and *s* assignment in the HH' region is proposed on the basis of the work reported herein.



selection of *rac*-PO and *S*-PO, we can determine the stereochemical sequences in the etherols. Then in the reaction with triphosgene by combinations of etherols derived from *S*-PO and *rac*-PO, we obtained carbonates containing statistical (*i* + *s*) and enriched (*i*) stereo-sequences.

NMR Spectra and Assignments. The $^{13}\text{C}\{^1\text{H}\}$ signals of the carbonate carbon for $n = 1$ and 2 are

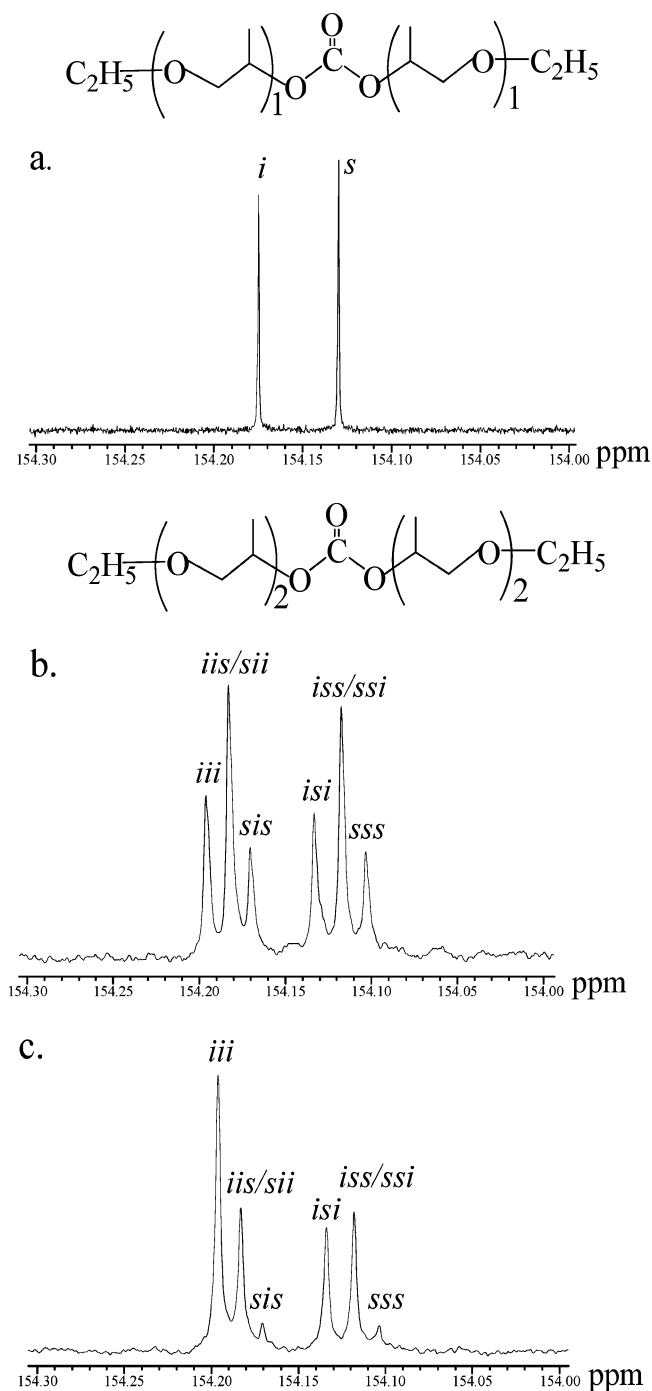


Figure 2. $^{13}\text{C}\{^1\text{H}\}$ (150 MHz, CDCl_3) NMR spectra of carbonate carbon region of regioregular oligoether carbonate compounds ($n = 1, 2$). Carbonate compounds in (b) were made from etherol derived from *rac*-PO, while the ones in (c) were prepared from etherol mixtures (1:1) derived separately from *rac*-PO and *S*-PO.

shown in Figure 2. For $n = 2$, it is clear that the ^{13}C carbonate signal shows tetrad sensitivity, and furthermore, since this molecule has a regiosequence (TH)(TH)·(HT)(HT) (H = methine group; T = methylene group), the signal for *iis* and *sii* cannot be distinguished. Similarly, the *ssi* and *iss* sequence is the same.

The spectra for $n = 3$ and 4 are shown in Figure S2 of the Supporting Information. For $n = 3$, there are 20 possible stereosequences, but no more than 12 signals are partially resolved. Thus, for $n \geq 4$ we can only assign the signal at the diad level, *i* or *s*. The spectra obtained for polyether carbonates $\text{Et}(\text{PO})_n\text{OCO}_2(\text{PO})_n\text{Et}$, where

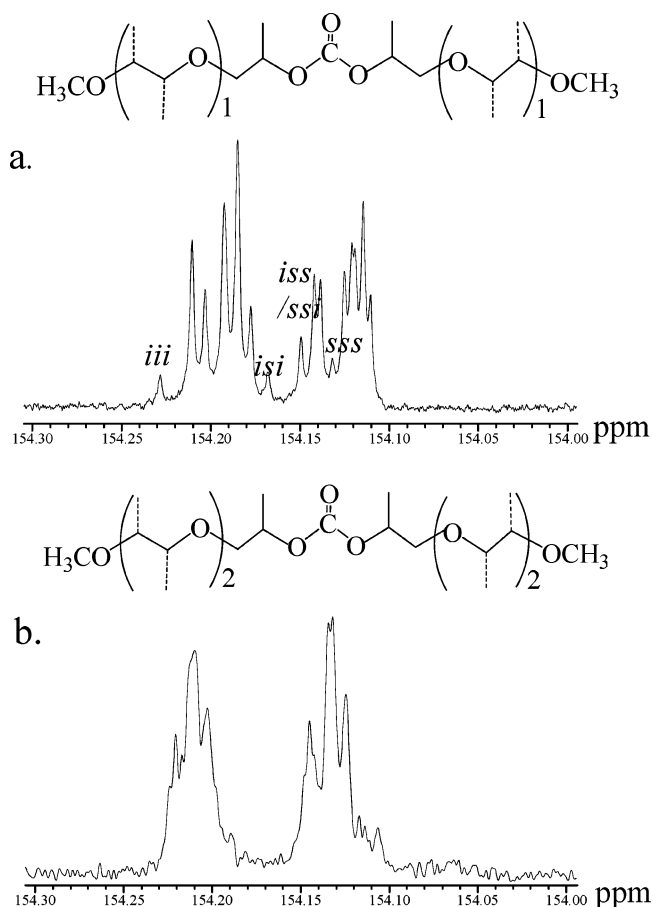


Figure 3. $^{13}\text{C}\{^1\text{H}\}$ (150 MHz, CDCl_3) NMR spectra of carbonate carbon region of regioirregular oligoether carbonate compounds ($n = 1, 2$).

$n = \sim 10$ and ~ 30 , are shown in Figure S3. These spectra further demonstrate that only diad sensitivity is seen.

From the use of commercial sources of regioirregular etherols, $\text{CH}_3(\text{PO})_n(\text{OCH}_2\text{CHMe})\text{OH}$, where $n = 1$ and 2, we have made ether carbonates that have HH junctions at the carbonate carbon but are otherwise regioirregular. The $^{13}\text{C}\{^1\text{H}\}$ spectra of the carbonate carbon are shown in Figure 3. For $n = 1$, we observed tetrad sensitivity and can identify the stereosequences associated with the regioregular component (see Supporting Information for details). Once again, however, as the chain length increases on each side of the carbonate, the sensitivity is reduced so that only *i* and *s* regions can be unequivocally identified. Finally, we should note that the chemical shift difference between the unique resonances is quite small, typically less than 0.1 ppm.

Structural Considerations. As an aid to the interpretation of the NMR data, we have employed calculations using density functional theory (DFT)¹⁶ and the Gaussian 98 suite of programs¹⁷ to examine the energies of various conformers. As a starting point, we examined dimethyl carbonate, MeOCO_2Me , which can exist in three local minima, namely *cis-cis*, *trans-trans*, and *cis-trans* conformers as shown in A, B, and C below, respectively. Experimentally, it is known that *cis-cis* is thermodynamically preferred, and a related carbonate molecule has been structurally characterized by single-crystal crystallography in this *cis-cis* geometry.¹⁸ Previous DFT calculations, analogous to the ones reported here, also have revealed the preference for the *cis-cis*

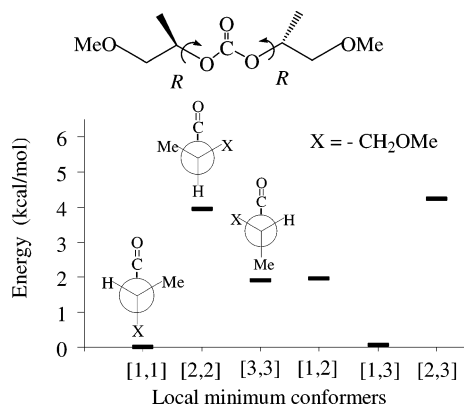


Figure 4. Six local minimum conformers in the gas-phase calculations for *RR* isomers of $\text{MeOCH}_2\text{CHMeOCO}_2\text{CHMeCH}_2\text{-OMe}$.

geometry, and our results closely parallel these earlier calculations.¹⁹ The *cis-trans* isomer is calculated to be higher in energy by 3.0 kcal/mol while the *trans-trans* is higher by 21.1 kcal/mol. On the basis of these energy differences, the *cis-cis* isomer will constitute more than 99% of the mixture at room temperature, 298 K. Consequently, we started our calculations of the compounds $\text{MeOCH}_2\text{CHMeOCO}_2\text{CHMeCH}_2\text{OMe}$ with the *cis-cis* geometry.

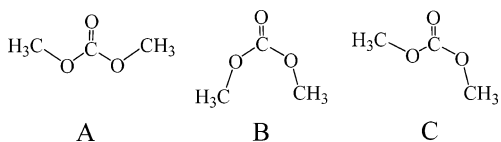


Figure 5. Six local minimum conformers in the gas-phase calculations for *SR* isomers of $\text{MeOCH}_2\text{CHMeOCO}_2\text{CHMeCH}_2\text{-OMe}$.

The *SR* isomers are compared in Figure 5 for the *cis-cis* geometry about the carbonate. Again we show the calculated local minima, and here for the conformers [1,1], [2,2], and [3,3], there is C_s symmetry but for all others only C_1 . In the Newman projections, we show only the *S* half of the molecule. Once again the MeO groups are *anti* to the carbonate O-CHMe bond. For the *SR* case, the gas-phase structures of the [1,1], [1,3], and [3,3] conformers are very close in energy, differing by less than 0.15 kcal/mol, indicating that these would be the dominant species in equilibrium at 298 K.

We also investigated the solvent effects on the preferred conformations of the methoxy-terminated oligomers using the polarizable continuum model (PCM) in our calculations,²⁰ and their respective energies in chloroform and benzene differed little from those calculated for the gas phase. These energies are compared in Table 1. This suggests that the dominant species present in the gas phase also exist in chloroform and benzene predominantly.

The results of the gas-phase calculations for the *RR* isomer, the molecule with the isotactic carbonate HH junction, are summarized in Figure 4. The conformations depicted in Figure 4 are viewed down the C-O bond of the carbonate, and all of these conformers represent local minima as confirmed by vibrational frequency analyses. The nomenclature for the calculated six minima indicates whether or not the molecule has C_2 or C_1 symmetry. Thus, structures [1,1], [2,2], and [3,3] have C_2 symmetry whereas the combinations [2,3], [1,3], and [1,2] contain two different halves on either side of the molecule and have C_1 symmetry. In the latter cases, only the gross geometry of the 1, 2, or 3 fragment is present in the respective [1,1], [2,2], or [3,3] isomer. The bond angles and bond lengths are fully optimized for each structure. On the basis of these gas-phase structures, we can estimate that [1,1] and [1,3] isomers constitute >95% of the species present at 298 K, and the [3,3] and [1,2] isomers are less than 2% each. The structures depicted in Figure 4 all have an *anti* conformation of the ether oxygen with respect to the carbonate O-CHMe bond as shown. The *gauche* conformer is higher in energy by 0.94 kcal/mol in the case of the [1,1] isomer.

The molecules of $\text{MeOCO}_2\text{CH}_2\text{CHMeOCO}_2\text{CHMeCH}_2\text{-OCO}_2\text{Me}$, considered as a small segment of the PPC chain, were also investigated in our calculations. The results of the calculations for *RR* isomers in both the gas phase and chloroform are summarized in Figure 6. Because of the huge number of all possible conformations, we simplified the calculations by only dealing with the ones having C_2 symmetry derived from [1,1] in Figure 4 and keeping all three carbonate groups in the *cis-cis* conformation. The Newman projections depicted in Figure 7 are viewed down the bonds of CH(Me)-O (1), CH₂-CH(Me) (2), and O-CH₂ (3). The nomenclature for the calculated six minima in Figure 6 indicates a combination of those three views. For example, [1,3',2''] represents that a half of this isomer has conformation 1 for the CH(Me)-O bond, 3' for the CH₂-CH(Me), and 2'' for the O-CH₂, and the entire isomer has a C_2 symmetry. The bond angles and lengths are fully optimized. The relative energies of the six isomers are in the range 0–1.1 kcal/mol as shown in Figure 6, which

Table 1. Calculated Populations for the Isomers of $\text{MeOCH}_2\text{CHMeOCO}_2\text{CHMeCH}_2\text{OMe}$ in the Gas Phase, Chloroform, and Benzene

conformers	gas phase		chloroform		benzene		
	ΔE (kcal/mol)	population ratio	ΔE (kcal/mol)	population ratio	ΔE (kcal/mol)	population ratio	
<i>RR</i>	[1,1]	0	1	0	1	0	1
	[1,3]	0.050	0.918	0.077	0.879	0.056	0.909
<i>SR</i>	[1,1]	0.010	1	0.004	1	0.012	1
	[3,3]	0.131	0.815	0.080	0.880	0.099	0.863
	[1,3]	0.027	0.971	0.005	0.998	0.014	0.997

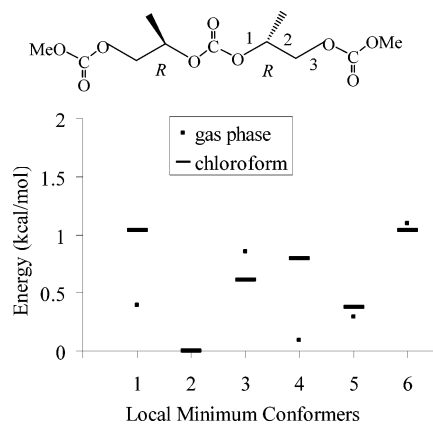


Figure 6. Six local minimum conformers in both the gas phase and chloroform calculations for *RR* isomers having C_2 symmetry of $\text{MeOCO}_2\text{CH}_2\text{CHMeOCO}_2\text{CHMeCH}_2\text{OCO}_2\text{Me}$. The conformers' structures are according to Figure 7: 1, [1,1',1'']; 2, [1,2',2'']; 3, [1,3',1'']; 4, [1,1',2'']; 5, [1,2',2'']; 6, [1,3',2''].

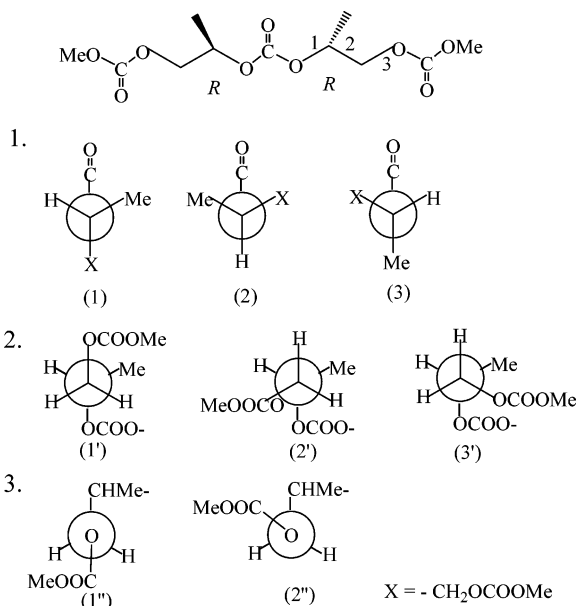


Figure 7. Newman projections for the *RR* isomers of $\text{MeOCO}_2\text{CH}_2\text{CHMeOCO}_2\text{CHMeCH}_2\text{OCO}_2\text{Me}$, viewing down the bonds of $\text{CH}(\text{Me})-\text{O}$, $\text{CH}_2-\text{CH}(\text{Me})$, and $\text{O}-\text{CH}_2$.

indicates that all of them have contributions more or less to the Boltzmann average at 298 K. The relative energies for some isomers in chloroform differ significantly from the gas phase, in contrast to the molecules of $\text{MeOCH}_2\text{CHMeOCO}_2\text{CHMeCH}_2\text{OME}$, which suggests that solvent effects will play a more important role on the conformations of this molecule.

The *SR* isomers of $\text{MeOCO}_2\text{CH}_2\text{CHMeOCO}_2\text{CHMeCH}_2\text{OCO}_2\text{Me}$ are compared in Figure 8. Again, we only show the results of symmetric conformers (C_s) derived from [1,1] and [3,3] in Figure 5. We began with many initial starting geometries, but some potential structures optimized to a reduced number of final geometries. Indeed, we obtained eight minima in the relative energy range 0–1.7 kcal/mol. Similarly to *RR* isomers, the relative energies for some *SR* isomers in chloroform were much different from the gas phase, as shown in Figure 8.

NMR Calculations. With an attempt to simulate the ^{13}C NMR chemical shifts of central carbonate carbons of the model compounds, we carried out NMR calculations employing the gauge-independent atomic orbital

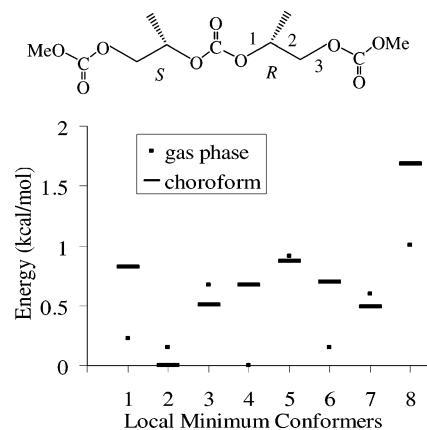


Figure 8. Eight local minimum conformers in both the gas phase and chloroform calculations for *SR* isomers having C_s symmetry of $\text{MeOCO}_2\text{CH}_2\text{CHMeOCO}_2\text{CHMeCH}_2\text{OCO}_2\text{Me}$. The structures of conformers are as follows: 1, [1,1',1'']; 2, [1,2',2'']; 3, [1,3',1'']; 4, [1,1',2'']; 5, [1,3',2'']; 6, [3,1',1'']; 7, [3,3',1'']; 8, [3,1',2''].

Table 2. Calculated NMR Chemical Shifts for the Isomers of $\text{MeOCH}_2\text{CHMeOCO}_2\text{CHMeCH}_2\text{OME}$ in the Gas Phase and Chloroform

conformers	gas phase (ppm)	chloroform (ppm)	
<i>RR</i>	[1,1]	162.529	162.345
	[1,3]	162.820	162.675
	ave ^a	162.668	162.499
<i>SR</i>	[1,1]	162.429	162.377
	[3,3]	163.352	163.062
	[1,3]	162.903	162.662
ave	162.864	162.685	
<i>RR-SR</i> ^b	-0.196	-0.186	

^a Statistical average chemical shift. ^b Chemical shift difference between *RR* and *SR*.

(GIAO) method available in Gaussian.²¹ For the molecules of $\text{MeOCH}_2\text{CHMeOCO}_2\text{CHMeCH}_2\text{OME}$, the results are tabulated in Table 2. For the *RR* isomer, two carbonate carbon signals are predicted at 162.345 and 162.675 ppm in chloroform for the predominant local minima. Given that at room temperature rotations about single bonds will be rapid on the NMR time scale, this predicts a single carbonate carbon resonance at 162.499 ppm. For the *SR* isomer where three local minima are predicted to contribute to the average carbon resonance of the carbonate carbon in chloroform, we find 162.377, 163.062, and 162.662 ppm. Given the relative population of these conformers at 298 K (1:0.880:0.998), the predicted carbonate carbon signal is 162.685 ppm. The calculated chemical shift separation for the carbonate carbon signals of the two isomers representing *i* and *s* junctions is 0.186 ppm, which may be compared to 0.042 ppm in CDCl_3 solution. Moreover, the calculations predict that the *RR* isomer should have a chemical shift upfield relative to the *SR* isomers, which is contrary to our experimental assignment in the model compounds (with the ethoxy end groups) for *i* and *s*. It is probably unreasonable to expect our current level of computation of NMR chemical shifts to simulate with accuracy such small experimental variations. For instance, the concentration of the solution (0.2 M CDCl_3 solution used in NMR experiments), not simulated in the calculations, may have significant effects on the intermolecular chain interactions, which changes the relative energies and populations of the conformations and results in deviations in the calculated NMR chemical shifts from the experimental ones. However, the

Table 3. Calculated NMR Chemical Shifts for the Isomers of MeOCO₂CH₂CHMeOCO₂CHMeCH₂OCO₂Me in the Gas Phase and Chloroform

conformers		gas phase (ppm)	chloroform (ppm)	
<i>RR</i>	[1,1',1'']	162.307	162.127	
	[1,2',1'']	163.052	162.879	
	[1,3',1'']	163.257	162.968	
	[1,1',2'']	161.967	160.488	
	[1,2',2'']	163.436	163.665	
	[1,3',2'']	163.291	162.695	
	ave ^a	162.761	162.741	
	<i>SR</i>	[1,1',1'']	162.468	161.976
		[1,2',1'']	162.995	161.951
		[1,3',1'']	163.233	162.645
[1,1',2'']		161.941	161.510	
[1,3',2'']		163.167	162.336	
[3,1',1'']		163.093	162.664	
[3,3',1'']		163.508	162.341	
[3,1',2'']		163.252		
ave	162.766	162.167		
<i>RR-SR</i> ^b		-0.005	0.574	

^a Statistical average chemical shift. ^b Chemical shift difference between *RR* and *SR*.

calculations do indicate that the conformations of molecules and the configurations of stereocenters can make differences in chemical shifts. Consistently, it is experimentally evident from Figure 2 that the carbonate carbon is sensitive to the stereocenters of the ring-opened PO units in a chain of the type R(PO)_{*n*}OCO₂(PO)_{*n*}R, where *n* = 2. For *n* > 2, the rapidly increasing number of stereoisomers leads to overlapping resonances, and only diad sensitivity can be claimed by ¹³C NMR spectroscopy. In the case of longer chain molecules, such as R(PO)₁₀OCO₂(PO)₁₀R and R(PO)₃₀OCO₂(PO)₃₀R, only single broad resonances assignable to *i* and *s* are observed (see Supporting Information, Figure S3.) For the isotactic oligomer prepared from *S*-PO, the half-width of the signal for *i* is less than 0.01 ppm for *n* ~ 10. This is not significantly broader than the half-width seen for the *iii* tetrad signal where *n* = 2, which indicates that the time averaging of various conformers in the long chain oligomer remains fast on the NMR time scale.

The NMR chemical shifts for MeOCO₂CH₂CHMeOCO₂CHMeCH₂OCO₂Me were also calculated, and the results are tabulated in Table 3. In the gas phase, for *RR* isomers, the average central carbonate carbon signal is predicted at 162.761 ppm, while for the *SR* isomers, it is 162.766 ppm. In chloroform, the predicted chemical shifts for the central carbonate carbon are 162.741 ppm for *RR* and 162.167 ppm for *SR*.

Conclusions

The model compounds, R(PO)_{*n*}OCO₂(PO)_{*n*}R, where R = Me, Et, or H, and *n* = 1, 2, 3, 4, ~10, and ~30, were synthesized for PPC microstructural assignments in NMR studies. The ¹³C{¹H} NMR investigations of those compounds showed that the carbonate carbon signals have both regio- and stereosensitivity at the diad and the tetrad levels to its adjacent PO ring-opened units. The calculations on the model compounds indicated that the carbonate groups exist predominantly at *cis-cis* geometries with more than one stable conformation for each molecule. In addition, the ¹³C chemical shifts predicted in the calculations were sensitive to the conformations of the molecules and the configurations of the stereocenters in PO ring-opened units.

Experimental Section

All syntheses and solvent manipulations were carried out under a nitrogen atmosphere using standard Schlenk-line and drybox techniques. Solvents were distilled from sodium benzophenone ketyl. Racemic propylene oxide (Fisher) and *S*-propylene oxide (Alfa Aesar) were distilled from calcium hydride. Potassium ethoxide (Aldrich), triphosgene (Aldrich), and anhydrous 1,4-dioxane (Aldrich) were used as received. Di- and tri(propylene glycol) methyl ethers (Aldrich), poly(propylene glycol) (typical *M_n* = 425) (Aldrich), and deuterated solvents were stored over 4 Å molecular sieves for 24 h prior to use.

NMR Experiments. ¹H and ¹³C{¹H} NMR experiments were carried out with a Bruker DRX-500 (5 mm broad band probe) and a Bruker DRX-600 (5 mm broad band probe) spectrometers, operating at proton Larmor frequencies of 500 and 600 MHz, respectively. The parameters used in ¹³C{¹H} NMR experiments on a Bruker DRX-600 spectrometer were as follows: number of data point, TD = 65 536; sweep width, SWH = 1502 Hz; relaxation time, D1 = 2 s; and chemical shift range 0–200 or 150–160 ppm. Typically 0.2 M sample solutions in chloroform-*d* were used in the analyses. Their peak frequencies were referenced against the solvent, chloroform-*d* at 7.24 ppm for ¹H and 77.0 ppm for ¹³C{¹H} NMR.

Mass Spectrometry. The polymer samples obtained in the reactions of polypropylene glycols and triphosgene were analyzed by matrix-assisted laser desorption/ionization time-of-flight mass spectrometry (MALDI-TOF/MS). MALDI-TOF was performed on a Bruker Reflex III (Bruker, Bremen, Germany) mass spectrometer operated in a linear, positive ion mode with a N₂ laser. Laser power was used at the threshold level required to generate signal. The accelerating voltage was set to 28 kV. The instrument was calibrated with protein standards bracketing the molecular weights of the samples. The 2,5-dihydroxybenzoic acid (DHBA) matrix was prepared as saturated solutions in THF. Allotments of 10 mL of matrix and 2 mL of a solution of the sample were thoroughly mixed together; 0.5 mL of this was spotted on the target plate and allowed to dry.

Small molecular weight di-, tri-, and tetra(propylene glycol) ethyl ethers and the carbonates produced from them were analyzed on a Bruker Esquire ion trap mass spectrometer (Bremen, Germany) equipped with an orthogonal electrospray source operated in positive ion mode. Samples were prepared in a solution containing methanol/acetic acid (99:1) and infused into the electrospray source at a rate of 5–10 mL/min. Optimal ESI conditions were as follows: capillary voltage, 3500 V; source temperature, 250 °C; the ESI drying gas, nitrogen. The ion trap was set to pass ions from *m/z* 50 to 2000 amu. Data were acquired in continuum mode until acceptable averaged data were obtained.

Chromatography. Gel permeation chromatographic (GPC) analysis was performed at 35 °C on a Waters Breeze system equipped with a Waters 410 refractive index detector and a set of two columns, Waters Styragel HR-2 and HR-4 (Milford, MA). THF (HPLC grade) was used as the mobile phase at 1.0 mL/min. The sample concentration was 0.1%, and the injection volume was 100 μL. The samples were centrifuged and filtered before analysis. The calibration curve was made with six polystyrene standards covering the molecular weight range from 580 to 460 000 Da. High-performance liquid chromatographic (HPLC) analysis was performed on the same instrument as GPC. Instead, a Symmetry C₁₈ (4.6 × 150 mm) column (Milford, MA) and methanol/water (50:50) mobile phase at 1.0 mL/min were used.

Calculations. The calculations were performed with density functional theory and the Gaussian 98 suite of programs.^{16,17} The geometry optimizations and vibrational frequency calculations were carried out at the B3LYP/6-31G(d) level.²² The calculations for NMR chemical shift prediction were done with the GIAO method and at the B3LYP/6-311+G-(2d,p) level in both the gas phase and with the PCM method for chloroform, using the optimized geometries of each local minimum.^{20,21}

Synthesis of Oligo(propylene glycol) Ethyl Ethers. In a typical reaction, potassium ethoxide (2.0 g, 23.8 mmol) was allowed to react with *rac*-PO (or *S*-PO) (5 mL, 71.6 mmol) in 40 mL of 1,4-dioxane at 90 °C for 20 h. After cooling to room temperature, the product was allowed to react with excess HCl solution. The solvents and any other volatile species were evaporated under vacuum. The residue was extracted with hexane. After hexane was distilled out, a yellow liquid was obtained, which was a mixture of oligo(propylene glycol) ethyl ethers. This mixture was separated using spinning band column distillation under vacuum at elevated temperatures to obtain pure (>98%) di-, tri-, and tetra(propylene glycol) ethyl ethers (colorless liquids). The final products were analyzed by HPLC, ESI/MS, and NMR.

Di(rac-propylene glycol) Ethyl Ether. ESI/MS: peak at m/z = 185 for $\text{Et}(\text{PO})_2\text{OH}\cdot\text{Na}^+$. ^1H NMR (CDCl_3 , δ , ppm): 0.97 (m, $2\text{CH}_3\text{-CH}$), 1.06 (t, $\text{CH}_3\text{-CH}_2$), 3.78 (m, CH-OH), 3.00–3.60 (m, CH_2 , CH , OH). ^{13}C $\{^1\text{H}\}$ NMR (CDCl_3 , δ , ppm): 14.76, 14.78, 16.22, 16.94, 18.00, 18.26 (CH_3), 66.42, 66.44, 74.16, 74.26, 75.53 (CH_2), 65.44, 66.88, 74.19, 75.94 (CH).

Tri(rac-propylene glycol) Ethyl Ether. ESI/MS: peak at m/z = 243 for $\text{Et}(\text{PO})_3\text{OH}\cdot\text{Na}^+$. ^1H NMR (CDCl_3 , δ , ppm): 0.90–1.10 (m, 4CH_3), 3.77 (m, CH-OH), 3.00–3.60 (m, CH_2 , CH , OH). ^{13}C $\{^1\text{H}\}$ NMR (CDCl_3 , δ , ppm): 14.84, 14.87, 14.88, 14.91, 16.68, 16.70, 16.78, 16.81, 16.86, 16.88, 16.94, 16.99, 18.00, 18.03, 18.30 (CH_3), 66.42, 66.43, 72.92, 73.04, 73.06, 73.13, 74.14, 74.23, 74.31, 74.34, 75.67 (CH_2), 65.31, 65.38, 66.87, 66.91, 74.47, 74.63, 74.90, 74.91, 74.98, 75.00, 76.24, 76.50 (CH).

Tetra(rac-propylene glycol) Ethyl Ether. ESI/MS: peak at m/z = 301 for $\text{Et}(\text{PO})_4\text{OH}\cdot\text{Na}^+$. ^1H NMR (CDCl_3 , δ , ppm): 0.90–1.10 (m, 4CH_3), 3.77 (m, CH-OH), 3.00–3.60 (m, CH_2 , CH , OH). ^{13}C $\{^1\text{H}\}$ NMR (CDCl_3 , δ , ppm): 14.78, 14.81, 14.82, 14.85, 16.62, 16.64, 16.67, 16.69, 16.72, 16.74, 16.79, 16.81, 16.84, 16.87, 17.97, 17.99, 18.00, 18.02 (CH_3), 66.32, 66.36, 72.63, 72.67, 72.83, 72.85, 72.87, 72.92, 72.96, 72.99, 73.05, 73.19, 73.21, 74.08, 74.12, 74.14, 74.16, 74.18, 74.25, 74.28, 75.54, 75.59, 75.61 (CH_2), 65.26, 65.31, 65.34, 66.77, 66.82, 74.41, 74.45, 74.57, 74.60, 74.75, 74.77, 74.83, 74.84, 74.89, 74.91, 74.93, 74.97, 75.03, 75.10, 75.16, 75.18, 76.14, 76.24, 76.26, 76.29, 76.30, 76.39 (CH).

Di(S-propylene glycol) Ethyl Ether. ESI/MS: peak at m/z = 185 for $\text{Et}(\text{PO})_2\text{OH}\cdot\text{Na}^+$. ^1H NMR (CDCl_3 , δ , ppm): 0.97 (m, $2\text{CH}_3\text{-CH}$), 1.06 (t, $\text{CH}_3\text{-CH}_2$), 3.78 (m, CH-OH), 3.00–3.60 (m, CH_2 , CH , OH). ^{13}C $\{^1\text{H}\}$ NMR (CDCl_3 , δ , ppm): 14.89, 16.76, 18.29 (CH_3), 66.53, 74.31, 74.38 (CH_2), 65.50, 74.29 (CH).

Tri(S-propylene glycol) Ethyl Ether. ESI/MS: peak at m/z = 243 for $\text{Et}(\text{PO})_3\text{OH}\cdot\text{Na}^+$. ^1H NMR (CDCl_3 , δ , ppm): 0.90–1.10 (m, 4CH_3), 3.77 (m, CH-OH), 3.00–3.60 (m, CH_2 , CH , OH). ^{13}C $\{^1\text{H}\}$ NMR (CDCl_3 , δ , ppm): 15.01, 16.79, 17.01, 18.32 (CH_3), 66.57, 73.17, 74.31, 74.44 (CH_2), 65.48, 74.55, 75.12 (CH).

$\text{C}_2\text{H}_5\text{-[OCH}_2\text{CH(CH}_3\text{)]}_n\text{-OH}$ (Average n = 10). Potassium ethoxide (0.24 g, 2.86 mmol) was reacted with *rac*-PO (or *S*-PO) (2 mL, 28.6 mmol) in 20 mL of 1,4-dioxane at 90 °C for 20 h. After the addition of HCl solution, removal of solvents and extraction with hexane, a yellow liquid was obtained (90% yield). Using *rac*-PO: GPC, M_n = 740, PDI = 1.28. ^1H NMR (CDCl_3 , δ , ppm): 0.90–1.10 (m, CH_3), 3.83 (m, CH-OH), 3.00–3.60 (m, CH_2 , CH , OH). ^{13}C $\{^1\text{H}\}$ NMR (CDCl_3 , δ , ppm): 15.02–18.63 (m, CH_3), 67.01, 73.30–74.90, 76.24, 76.32 (CH_2), 65.95, 65.98, 67.51, 67.57, 75.08–75.90, 77.46 (CH). Using *S*-PO: GPC, M_n = 780, PDI = 1.25. ^1H NMR (CDCl_3 , δ , ppm): 0.90–1.10 (m, CH_3), 3.83 (m, CH-OH), 3.00–3.60 (m, CH_2 , CH , OH). ^{13}C $\{^1\text{H}\}$ NMR (CDCl_3 , δ , ppm): 15.46–19.20 (m, CH_3), 73.00, 73.08, 73.13, 74.17, 74.18 (CH_2), 65.27, 66.30, 74.38, 74.84, 75.13, 75.16, 75.20 (CH).

$\text{C}_2\text{H}_5\text{-[OCH}_2\text{CH(CH}_3\text{)]}_n\text{-OH}$ (Average n = 50). This large MW polymer sample was synthesized to investigate the regio- and stereoselectivity of PO ring-opening in the above reactions (see Supporting Information). Potassium ethoxide (24 mg, 0.29 mmol) was allowed to react with *rac*-PO (2 mL, 28.6 mmol) in the same condition and following the same procedure as above. A yellow viscous liquid was finally yielded. GPC: M_n = 5040, PDI = 1.32. ^1H NMR (CDCl_3 , δ , ppm): 0.90–1.10 (m, CH_3),

3.83 (m, CH-OH), 3.00–3.60 (m, CH_2 , CH , OH). ^{13}C $\{^1\text{H}\}$ NMR (CDCl_3 , δ , ppm): 17.71, 17.83 (CH_3), 72.73, 72.78, 72.86, 72.99, 73.23, 73.26 (CH_2), 74.99, 75.18, 75.22, 75.37 (CH).

Synthesis of Model Carbonate Compounds. $\text{R-(PO)}_n\text{-OCOO-(PO)}_n\text{-R}$, $\text{R} = \text{CH}_3$, C_2H_5 , or H , were synthesized as following. $\text{R-(PO)}_n\text{-OH}$ (0.5 mL) was reacted with 1/6 molar equivalent of triphosgene in 2 mL of benzene, stirring.¹⁵ After 3 h, 2 mL of pyridine was added into the flask, and the temperature was increased to 60 °C for another 12 h. After the removal of solvent and volatile species, the product was extracted with hexane. The final products were analyzed with MS and NMR.

$\text{CH}_3(\text{PO})_2\text{OH/Triphosgene}$. ESI/MS: peak at m/z = 373 for $\text{Me}(\text{PO})_2\text{OCO}_2(\text{PO})_2\text{Me}\cdot\text{Na}^+$. ^1H NMR: 1.00–1.30 (m, $\text{CH}_3\text{-CH}$), 3.10–3.60 (m, $\text{CH}_3\text{-O}$, CH_2 , CH), 4.86 (m, CH-OCO_2). ^{13}C $\{^1\text{H}\}$ NMR: 16.83–17.43 ($\text{CH}_3\text{-CH}$), 57.18, 59.52 ($\text{CH}_3\text{-O}$), 71.67, 71.69, 71.75, 72.05, 72.10, 73.95, 74.01, 74.06, 75.46, 75.49, 77.00, 77.13 (CH_2), 73.51–73.90, 74.09, 74.15, 75.66, 75.68, 76.28 (CH), 154.10–154.25 (C=O).

$\text{CH}_3(\text{PO})_3\text{OH/Triphosgene}$. ESI/MS: peak at m/z = 489 for $\text{Me}(\text{PO})_3\text{OCO}_2(\text{PO})_3\text{Me}\cdot\text{Na}^+$. ^1H NMR: 1.05–1.30 (m, $\text{CH}_3\text{-CH}$), 3.20–3.70 (m, $\text{CH}_3\text{-O}$, CH_2 , CH), 4.87 (m, CH-OCO_2). ^{13}C $\{^1\text{H}\}$ NMR: 16.48–18.30 ($\text{CH}_3\text{-CH}$), 59.46 ($\text{CH}_3\text{-O}$), 71.50–73.85, 74.74, 74.83, 76.37–77.08 (CH_2), 73.87, 74.05, 74.15, 74.93–76.31 (CH), 154.10–154.25 (C=O).

$\text{CH}_3\text{CH}_2(\text{rac-PO})_1\text{OH/Triphosgene}$. ESI/MS: peak at m/z = 257 for $\text{Et}(\text{PO})_1\text{OCO}_2(\text{PO})_1\text{Et}\cdot\text{Na}^+$. ^1H NMR: 1.08 (t, $\text{CH}_3\text{-CH}_2$), 1.19 (m, $\text{CH}_3\text{-CH}$), 3.00–4.00 (m, CH_2 , CH), 4.82 (m, CH-OCO_2). ^{13}C $\{^1\text{H}\}$ NMR: 14.88, 16.49, 16.51 (CH_3), 66.53, 66.54, 72.54, 72.60 (CH_2), 73.13, 73.18 (CH), 154.13–154.18 (C=O).

$\text{CH}_3\text{CH}_2(\text{rac-PO})_2\text{OH/Triphosgene}$. ESI/MS: peak at m/z = 373 for $\text{Et}(\text{PO})_2\text{OCO}_2(\text{PO})_2\text{Et}\cdot\text{Na}^+$. ^1H NMR: 1.00–1.30 (m, CH_3), 3.00–3.60 (m, CH_2 , CH), 4.80 (m, CH-OCO_2). ^{13}C $\{^1\text{H}\}$ NMR: 15.00–17.20 (CH_3), 66.54 ($\text{CH}_3\text{-CH}_2\text{-O}$), 71.20, 71.26, 71.59, 71.62, 74.33, 74.37, 74.50 (CH_2), 73.34, 73.38, 73.51, 73.59, 75.10, 75.12, 75.34, 75.35 (CH), 154.09–154.20 (C=O).

$\text{CH}_3\text{CH}_2(\text{rac-PO})_3\text{OH/Triphosgene}$. ESI/MS: peak at m/z = 489 for $\text{Et}(\text{PO})_3\text{OCO}_2(\text{PO})_3\text{Et}\cdot\text{Na}^+$. ^1H NMR: 1.00–1.30 (m, CH_3), 3.00–3.60 (m, CH_2 , CH), 4.78 (m, CH-OCO_2). ^{13}C $\{^1\text{H}\}$ NMR: 15.00–18.30 (CH_3), 66.49 ($\text{CH}_3\text{-CH}_2\text{-O}$), 71.10–73.30, 74.20–74.40, 75.83 (CH_2), 73.31, 73.50, 73.58, 73.60, 74.42–75.62, 76.43 (CH), 154.10–154.21 (C=O).

$\text{CH}_3\text{CH}_2(\text{rac-PO})_4\text{OH/Triphosgene}$. ESI/MS: peak at m/z = 605 for $\text{Et}(\text{PO})_4\text{OCO}_2(\text{PO})_4\text{Et}\cdot\text{Na}^+$. ^1H NMR: 1.00–1.30 (m, CH_3), 3.10–3.60 (m, CH_2 , CH), 4.78 (m, CH-OCO_2). ^{13}C $\{^1\text{H}\}$ NMR: 15.00–17.30 (CH_3), 66.48 ($\text{CH}_3\text{-CH}_2\text{-O}$), 71.09–71.70, 72.80–73.25, 73.34, 73.38, 74.30–74.77 (CH_2), 73.27, 73.31, 73.49, 73.57, 73.59, 74.86–75.64 (CH), 154.08–154.20 (C=O).

50% $\text{CH}_3\text{CH}_2(\text{rac-PO})_2\text{OH}/50\% \text{CH}_3\text{CH}_2(\text{S-PO})_2\text{OH/Triphosgene}$. ESI/MS: peak at m/z = 373 for $\text{Et}(\text{PO})_2\text{OCO}_2(\text{PO})_2\text{Et}\cdot\text{Na}^+$. It has similar chemical shifts for the signals in ^1H and ^{13}C $\{^1\text{H}\}$ NMR spectra to the product of $\text{CH}_3\text{CH}_2(\text{rac-PO})_2\text{-OH/triphosgene}$, except that the relative intensities are different.

50% $\text{CH}_3\text{CH}_2(\text{rac-PO})_3\text{OH}/50\% \text{CH}_3\text{CH}_2(\text{S-PO})_3\text{OH/Triphosgene}$. ESI/MS: peak at m/z = 489 for $\text{Et}(\text{PO})_3\text{OCO}_2(\text{PO})_3\text{Et}\cdot\text{Na}^+$. It has similar chemical shifts for the signals in ^1H and ^{13}C $\{^1\text{H}\}$ NMR spectra to the product of $\text{CH}_3\text{CH}_2(\text{rac-PO})_3\text{-OH/triphosgene}$, except that the relative intensities are different.

$\text{CH}_3\text{CH}_2(\text{rac-PO})_n\text{OH}$ (Average n = 10)/Triphosgene. MALDI/MS: major series, $\text{Et}(\text{PO})_n\text{OCO}_2(\text{PO})_n\text{Et}\cdot\text{Na}^+$. ^1H NMR: 1.00–1.30 (m, CH_3), 3.00–3.60 (m, CH_2 , CH), 4.80 (m, CH-OCO_2). ^{13}C $\{^1\text{H}\}$ NMR: 16.60–18.40 (CH_3), 66.50 ($\text{CH}_3\text{-CH}_2\text{-O}$), 70.20–76.00 (CH_2 , CH), 154.08–154.20 (C=O).

$\text{CH}_3\text{CH}_2(\text{S-PO})_n\text{OH}$ (Average n = 10)/Triphosgene. MALDI/MS: major series, $\text{Et}(\text{PO})_n\text{OCO}_2(\text{PO})_n\text{Et}\cdot\text{Na}^+$. ^1H NMR: 1.00–1.30 (m, CH_3), 3.10–3.60 (m, CH_2 , CH), 4.78 (m, CH-OCO_2). ^{13}C $\{^1\text{H}\}$ NMR: 16.40–17.40 (CH_3), 66.45 ($\text{CH}_3\text{-CH}_2\text{-O}$), 71.50–75.80 (CH_2 , CH), 154.21 (C=O).

Poly(propylene glycol) (M_n = 2000)/Triphosgene. MALDI/MS: two major series, $\text{HO}(\text{PO})_n\text{OCO}_2(\text{PO})_n\text{OH}\cdot\text{Na}^+$, and $\text{HO}(\text{PO})_n\text{OCO}_2(\text{PO})_n\text{OCO}_2(\text{PO})_n\text{OH}\cdot\text{Na}^+$. ^1H NMR: 1.00–1.30 (m, CH_3), 3.10–3.60 (m, CH_2 , CH), 4.78 (m, CH-OCO_2). ^{13}C

$\{^1\text{H}\}$ NMR: 17.00–17.50 (CH₃), 72.50–73.40 (CH₂), 74.70–75.50 (CH), 154.10–154.22 (C=O).

Acknowledgment. We thank the Department of Energy, Office of Basic Sciences, Chemistry Division, for financial support of this work. We gratefully acknowledge generous computational resources from the Ohio Supercomputer Center where these calculations were performed. The mass spectrometers were purchased by a grant from the Hayes Investment Fund of the Ohio Board of Regents. We thank the staff of the Campus Chemical Instrument Center (CCIC) for running the samples by both NMR and MS techniques. We also thank Dr. Edward M. Dexheimer at BASF Corp., Dr. Wei Chen, and Dr. Meng-Lin Tsao at The Ohio State University for helpful discussion.

Supporting Information Available: $^{13}\text{C}\{^1\text{H}\}$ NMR (150 MHz, CDCl₃) spectrum of PPO obtained from PO polymerization with KOEt (50:1), showing the regio- and stereoselectivity involved in propylene oxide ring-opening polymerization; $^{13}\text{C}\{^1\text{H}\}$ (150 MHz, CDCl₃) NMR spectra of carbonate carbon region of regioregular oligoether carbonate compounds ($n = 3, 4$); statistical calculations for stereosequences of carbonate carbons in regioregular Et(PO)₂OCO₂(PO)₂Et and Et(PO)₃OCO₂(PO)₃Et made from etherol derived from *rac*-PO, as well as from etherol mixtures (1:1) derived separately from *rac*-PO and *S*-PO; statistical calculations for regio- and stereosequences of carbonate carbons in regioirregular Me(PO)₂OCO₂(PO)₂Me made from regioirregular di(propylene glycol) methyl ethers; and $^{13}\text{C}\{^1\text{H}\}$ (150 MHz, CDCl₃) NMR spectra of carbonate carbon region of regioregular oligoether carbonate compounds ($n = \sim 10, \sim 30$); energetic and coordinate information on the optimized geometries obtained in the calculations for dimethyl carbonate, MeOCH₂CHMeOCO₂CHMeCH₂OMe, and MeOCO₂CH₂CHMeOCO₂CHMeCH₂OCO₂Me. This material is available free of charge via the Internet at <http://pubs.acs.org>.

References and Notes

- (1) Darensbourg, D. J.; Holtcamp, M. W. *Coord. Chem. Rev.* **1996**, *153*, 155–174.
- (2) Super, M. S.; Beckman, E. J. *Trends Polym. Sci.* **1997**, *5*, 236–240.
- (3) Rokicki, A.; Kuran, W. *J. Macromol. Sci., Rev. Macromol. Chem. Phys.* **1981**, *C21*, 135–186.

- (4) Wilks, E. S. *Industrial Polymers Handbook*; Wiley-VCH: Weinheim, Germany, 2001; Vol. 1, pp 291–304.
- (5) Inoue, S.; Koinuma, H.; Tsuruta, T. *J. Polym. Sci., Polym. Lett.* **1969**, *7*, 287–292.
- (6) Ree, M.; Bae, J. Y.; Jung, J. H.; Shin, T. *J. Korea Polym. J.* **1999**, *7*, 333–349.
- (7) Allen, S. D.; Moore, D. R.; Lobkovsky, E. B.; Coates, G. W. *J. Am. Chem. Soc.* **2002**, *124*, 14284–14285.
- (8) Qin, Z.; Thomas, C. M.; Lee, S.; Coates, G. W. *Angew. Chem., Int. Ed.* **2003**, *42*, 5484–5487.
- (9) Darensbourg, D. J.; Yarbrough, J. C.; Ortiz, C.; Fang, C. C. *J. Am. Chem. Soc.* **2003**, *125*, 7586–7591.
- (10) Eberhardt, R.; Allmendinger, M.; Rieger, B. *Macromol. Rapid Commun.* **2003**, *24*, 194–196.
- (11) Chisholm, M. H.; Navarro-Llobet, D.; Zhou, Z. *Macromolecules* **2002**, *35*, 6494–6504.
- (12) Aida, T.; Ishikawa, M.; Inoue, S. *Macromolecules* **1986**, *19*, 8–13.
- (13) Steiner, E. C.; Pelletier, R. R. *J. Am. Chem. Soc.* **1964**, *86*, 4678–4686.
- (14) Chisholm, M. H.; Navarro-Llobet, D. *Macromolecules* **2002**, *35*, 2389–2392.
- (15) Eckert, H.; Forster, B. *Angew. Chem., Int. Ed. Engl.* **1987**, *26*, 894–895.
- (16) Parr, R. G.; Yang, W. *Density-Functional Theory of Atoms and Molecules*; Oxford University Press: Oxford, 1989.
- (17) Frisch, M. J.; Trucks, G. W.; Schlegel, H. B.; Scuseria, G. E.; Robb, M. A.; Cheeseman, J. R.; Zakrzewski, V. G.; Montgomery, J. A., Jr.; Stratmann, R. E.; Burant, J. C.; Dapprich, S.; Millam, J. M.; Daniels, A. D.; Kudin, K. N.; Strain, M. C.; Farkas, O.; Tomasi, J.; Barone, V.; Cossi, M.; Cammi, R.; Mennucci, B.; Pomelli, C.; Adamo, C.; Clifford, S.; Ochterski, J.; Petersson, G. A.; Ayala, P. Y.; Cui, Q.; Morokuma, K.; Malick, D. K.; Rabuck, A. D.; Raghavachari, K.; Foresman, J. B.; Cioslowski, J.; Ortiz, J. V.; Stefanov, B. B.; Liu, G.; Liashenko, A.; Piskorz, P.; Komaromi, I.; Gomperts, R.; Martin, R. L.; Fox, D. J.; Keith, T.; Al-Laham, M. A.; Peng, C. Y.; Nanayakkara, A.; Gonzalez, C.; Challacombe, M.; Gill, P. M. W.; Johnson, B. G.; Chen, W.; Wong, M. W.; Andres, J. L.; Head-Gordon, M.; Replogle, E. S.; Pople, J. A. *Gaussian 98*, revision A9; Gaussian, Inc.: Pittsburgh, PA, 1998.
- (18) Haque, M. U.; Caughlan, C. N.; Smith, G. D.; Ramirez, F.; Glaser, S. L. *J. Org. Chem.* **1976**, *41*, 1152–1154.
- (19) Bohets, H.; van der Veken, B. *J. Phys. Chem. Chem. Phys.* **1999**, *1*, 1817–1826.
- (20) Tomasi, J.; Persico, M. *Chem. Rev.* **1994**, *94*, 2027–2094.
- (21) Wiberg, K. B. *J. Comput. Chem.* **1999**, *20*, 1299–1303.
- (22) Becke, A. D. *Phys. Rev. A* **1988**, *38*, 3098–3100.

MA049850F